05

Progress of RFTES detector technology

© S.V. Shitov,[1,2] T.M. Kim,[1] L.S. Solomatov,[1] N.Yu. Rudenko,[1] A.V. Merenkov,[1] An.B. Ermakov,[2] V.I. Chichkov[1]

[1]National University of Science and Technology MISiS,
119049 Moscow, Russia
[2] Kotelnikov Institute of Radio Engineering and Electronics, Russian Academy of Sciences,
125009 Moscow, Russia
e-mail: Sergey3e@gmail.com

Received May 16, 2024
Revised May 16, 2024
Accepted May 16, 2024

The paper examines the current state of research and development of a new ultra-sensitive detection technology based on high-frequency heating of a superconducting microbridge by a combination of resonator currents at frequencies of about 1.5 GHz and a signal from a planar antenna in the frequency range 550−750 GHz at temperatures of 50−400 mK, called RFTES technology. The new technology aims to development of terahertz-range direct detectors of attowatt sensitivity and has already demonstrated performance close to theoretically possible under experimental conditions. A comparison with known superconducting detectors is made, competitive advantages and prospects for use in integrated circuits, including multi-element imaging arrays, are discussed, as well as the recently discovered strong kinetic effect in hafnium film at temperatures of about 100 mK. The prospects for the development of RFTES technology towards complex devices such as differential detectors and active integrated detectors with quantum sensitivity, as well as sources of thermodynamic noise for calibrating terahertz detectors with picowatt heat production are analyzed.

Keywords: direct detector, superconducting transition, superconducting microbridge, superconducting resonator, planar lens-antenna, RFTES, hafnium film, hot electron gas, RF superconductivity, thermodynamic noise, SQUID based RF amplifier, quantum sensitivity.

DOI: 10.61011/TP.2024.07.58802.168-24

Introduction

The development of a new technology for detection and visualization of superweak terahertz signals that was called Radio Frequency Transition Edge Sensor (RFTES) was aimed at making a detector that would combine the best properties of mature technologies such as TES (Transition Edge Sensor), MKID (Microwave Kinetic Inductance Detector), HEB (Hot Electron Bolometer) [1–8]. The name for the technology was chosen with reference to the established and internationally accepted English terminology, as applicable at that time, so the abbreviation RFTES will be used below. The basic operating principle of RFTES detector described in [9] was meant to be a new method for resistance measurement of a superconducting film in the vicinity of its critical temperature using the microwave resonator currents. Coaxial cables and a total absence of wires carrying direct current ensure high noise immunity of the measurement without using any special filters. The RFTES detector similar to the HEB detector has an absorber and thermometer combined in a single microbridge which allows the contradiction between bolometer sensitivity and quick response to be reduced dramatically. Such detector may be also called a HEB detector with microwave reading, but due to the essential part of innovative solutions and a wider range of applications described herein, it is reasonable to keep the traditional name RFTES.

A modern detector technology trend includes creation of imaging matrices where pixels are read via parallel channels to reduce the celestial mapping time due to the simultaneous signal integration. To protect against undesired heat, cooled detectors are combined into a matrix by the Frequency Domain Multiplexing Method (FDM) [6,10,11] using high-Q filters set to individual different frequencies which is one of the fundamental radio communications principle; thus, the resonator matrix may be read using a single physical channel — the coaxial cable, and in case of MKID and RFTES, a low-frequency SQUID amplifier may be replaced by a standard semiconductor microwave amplifier. The MKID technology uses the FDM method at frequencies about 10 GHz using planar superconducting resonators that serve as a band-stop filter, whose transmission is controlled by the nonlinear impedance Z_B of a film microabsorber as shown in Figure 1. This is a well-known radio engineering concept that has been used for almost half-century in frequency meters where mechanical variation of the resonator length makes it possible to find an unknown frequency by a narrow and deep minimum in power transmission [12]. The selective circuit using a planar band-stop filter (Figure 1) has universal applicability in a wide absorber impedance range Z_B and may be optimized for a distributed resonator. The bridge absorber, depending on its impedance, shall be inserted to different points on the distributed resonator because the current amplitude in such resonator varies along its length. Summing up all the above,

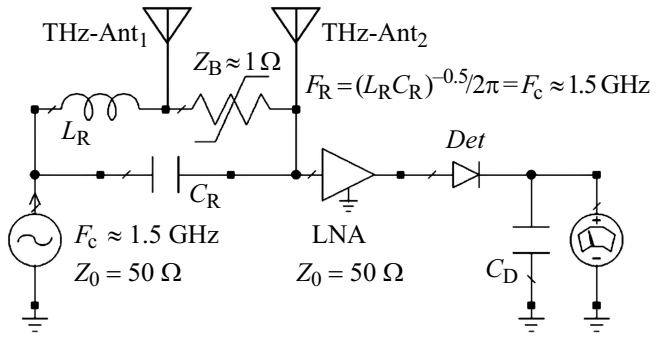

Figure 1. Conceptual equivalent circuit diagram of a receiver with RFTES detector. Operating principle — carrier modulation using a resonance band-stop filter at F_c by means of varying the band-stop filter Q factor. The antenna array (THz-Ant$_1$ and THz-Ant$_2$) provides directional reception of terahertz emission that warms up thermistor Z_B.

direct detectors running in the FDM mode are sounding signal modulators and, therefore, — dimensionless linear power transducers [W/W]. For this reason the signal transfer may be characterized in terms of the „power transfer ratio“ and „carrier modulation“. The direct power conversion to voltage or current (square-law detection) takes place in one of the last (buffer) stages of such receiver (*Det* — in Figure 1).

A detector constituting a HEB that operates at extremely low temperatures and has a record-breaking sensitivity of about $10^{-20}\,\mathrm{W}/\sqrt{\mathrm{Hz}}$ was described in [7]. Terahertz photon irradiation changed the resistance R of the Ti-based electron-gas microbridge near the critical microbridge temperature T_c and such response was measured with direct current using a SQUID amplifier. It was believed that measurement of such type of thermoresistive sensor using the FDM method at microwaves was most likely impossible or at least inefficient [13]. However, we have managed to develop a microbridge reading circuit from Hf using a microwave resonator and to demonstrate that it isn't so [14,15]. Value of the RFTES technology may be characterized as a combination of a maximum sensitivity with high stability and quick response that are sufficient to produce a high-performance direct detector that does not require any SQUID amplifier and allows integration into the imaging FDM matrix with reading frequencies about 1 GHz.

It is known that in the superconducting transition region the resistive component of non-linear microwave impedance prevails and RFTES matrix pixels, in contrast to the MKID matrix pixels, almost do not change their resonant frequency either when the carrier power varies or depending on the terahertz signal power increment, and are insensitive to the reference-frequency oscillator instability, thus, making their control easier. In addition, the frequency range of the received RFTES signals may extend from just a few GHz to far IR band, and the operating temperatures may be increased up to 400 mK [15] making sorption-pump cryostats suitable. These features will in future promote a wider application range of RFTES detectors as multipurpose sensors, including for fundamental research of terahertz cosmic radiation, in particular on board of space observatories. This study analyses the RFTES technology progress: brief history of creation, current status and some development prospects.

1. Experimental study at 4 K and 400 mK

Study of the new technology was started in collaboration with German colleagues at Karlsruhe university with building an electromagnetic all-niobium prototype to perform relatively simple experiments at liquid helium temperatures of about 4 K and to validate both the initial concept and the engineering approaches and analysis methods [14].

To receive the terahertz radiation from a black body at room temperature, an optical-window cryostat and a chip with 550−750 GHz integrated double-slot planar antenna were used (Figure 2). The resonance band-stop filter was designed using a quarter-wave segment of the coplanar waveguide with a frequency of about 5.4 GHz to implement the compact chip design. Interesting results were obtained already at the liquid helium temperatures and quite high practical sensitivity of the proposed detectors (Noise Equivalent Power, NEP) about $10^{-14}\,\mathrm{W}/\sqrt{\mathrm{Hz}}$ was demonstrated [16,17]. These studies have clearly shown the benefits of the new concept and the feasibility of cross-over to lower temperatures.

Tests at low and extremely low temperatures were started at National University of Science and Technology MISiS in 2014 where a set of RFTES prototypes using hafnium-film bridges was fabricated and passed preliminary test.

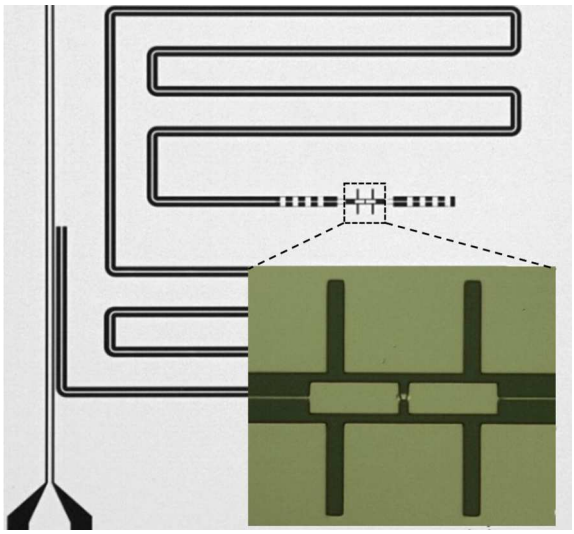

Figure 2. Photo of a chip with *C*-type RFTES detector. The magnified detail shows a terahertz double-slot antenna with a hafnium bridge in the center. A 1.5 GHz quarter-wave niobium resonator is folded for compactness. The bridge absorber is located near the open end of the resonator where the embedding impedance is about 1 Ohm.

The critical research stage included demonstration of high-frequency warm-up of the bridge by the reference (carrier) of about 1.5 GHz and smooth superconductivity suppression. Thermal conductivity measurements with substitution of the heat sink power by the carrier power keeping constant the Q factor showed that the electronic subsystem exhibits the electron gas properties within 100–300 mK [18].

The employed materials science approaches demonstrated thin (50–80 nm) films of hafnium with a critical temperature within 200–400 mK; bridges made from this material are technologically compatible with niobium microresonators Q $\sim$ 10 000 and exhibit microwave current nonlinearity very similar to that of the superconducting transition. At the next research stages, new testing methods were developed for RFTES detectors inside the dilution cryostat [19]. The bolometer response rate was measured using the method of warm-up the absorber at harmonics of the resonator; the experimentally measured response time was about 3 μs which agrees well with the high-Q resonator response time. It has been shown recently that the sensitivity of experimental chips agrees well with the theoretical predictions for electron-gas HEB detectors that are record-breaking to date, and features are described by original mathematical models that consider both the anomalous skin effect [20] in superconducting hafnium thin films and electrothermal feedback in the carrier circuits similar to [3]. Optical sensitivity of the experimental detectors was examined with the black-body source method within 550–750 GHz and a NEP value of about 10^{-17} W/$\sqrt{\text{Hz}}$ [15] was obtained and almost coincided with the theoretical prediction defined by the geometry of a particular prototype ($2 \times 2\,\mu$m bridge) and supported the feasibility of further efforts towards a sensitivity of about 10^{-20} W/$\sqrt{\text{Hz}}$ which is at the cosmic background noise level making the RFTES technology interesting for many other applied superconducting nanosystems. For successful development in this area, transition to submicron lithography of microbridges shall be planned, e.g. to $0.2 \times 0.2\,\mu$m, to increase the RFTES detector sensitivity by two orders of magnitude at once at the same operating temperatures.

2. Potential for reducing physical temperature of the detector

A method for achievement the nonlinear impedance at the carrier frequency is non-equilibrium warming conditions of the electronic subsystem near T_c that is an important part of the RFTES concept. We have reviewed the Mattis-Bardeen theory [20] provisions, which were used for critical assessment [21] of the new technology by predicting the degraded slope dR/dT of the superconducting transition measured at a high frequency. The argument was in that in the frequency region when the photon energy is close to the superconductor gap energy, $hf \approx 2\Delta$, the probability of full unpairing of superconducting carriers with photon absorption is close to 100% irrespective of temperature, i.e. current is induced by normal electrons; the same condition occurs near the critical temperature T_c, when the gap energy $\Delta(T_c) \to 0$, and, therefore, there shall be no temperature nonlinearity of the high-frequency impedance near T_c. According to this logic, reduction of T_c at the specified carrier frequency resulting in reduction of Δ shall additionally degrade the RFTES operation at extremely low temperatures. However, our numerical simulation using the Mattis-Bardeen results has shown that:

1) near T_c, $dT \cdot k_B \sim hf$ is satised, i.e. smearing of the superconducting transition temperature region dT is physically based on the shift of the effective electronic susbsystem temperature of the film by the temperature proportional to the carrier photon energy and weakly depends on a particular gap energy value if the gap energy at zero temperature is not too low, $\Delta(0) \gg hf$, which is shown by the data in Figure 3;

2) trend to the maximum slope is not a prerequisite for achievement of the fundamental sensitivity of the RFTES detector, which is supported bu electromagnetic calculations considering the „smeared“ dependences $R(T, f_c)$ [15].

The calculation shows that the superconducting transition slope dR/dT for the specified carrier frequency f_c and bridge resistance R_n depends weakly on Δ. This suggests that the employment of hafnium films with strong proximity effect may help promote the RFTES technology into the temperature region about 100 mK and below and, therefore, to reduce NEP proportionally to T^{-4}, i.e. more than by two orders of magnitude in transition from 400 mK to 100 mK while maintaining the same geometrical parameters of the bridge.

3. Kinetic effect

The main distinctive feature of the RFTES technology is a dissipative response of the bridge near T_c that is expressed in broadening the resonant absorption of the chip and reducing the strength of the absorption. However, minor shift of the resonance dip of the chip transmission ratio S21 still occurs [15]. This is explained by kinetic inductivity of the superconducting film when there is either low density of superconducting carriers or high density of high-frequency superconducting current that unpairs a considerable part of such carriers. In contrast to MKID, the kinetic induction may not play a significant role in the RFTES current transport where normal electrons locked within the bridge due to the Andreev mirrors [22] prevail, especially as the bridge is inserted in the low current region near the open end of the resonator as shown in Figure 2.

During the experimental studies, we tried to understand a seemingly collateral issue — some prototypes had no resonances. This could be explained by several reasons that shall be assigned to the known chip processing problems when the bottom absorber layer and top electrode film are applied with vacuum break. The consequences may be as follows: 1) insufficient quality of the hafnium film when

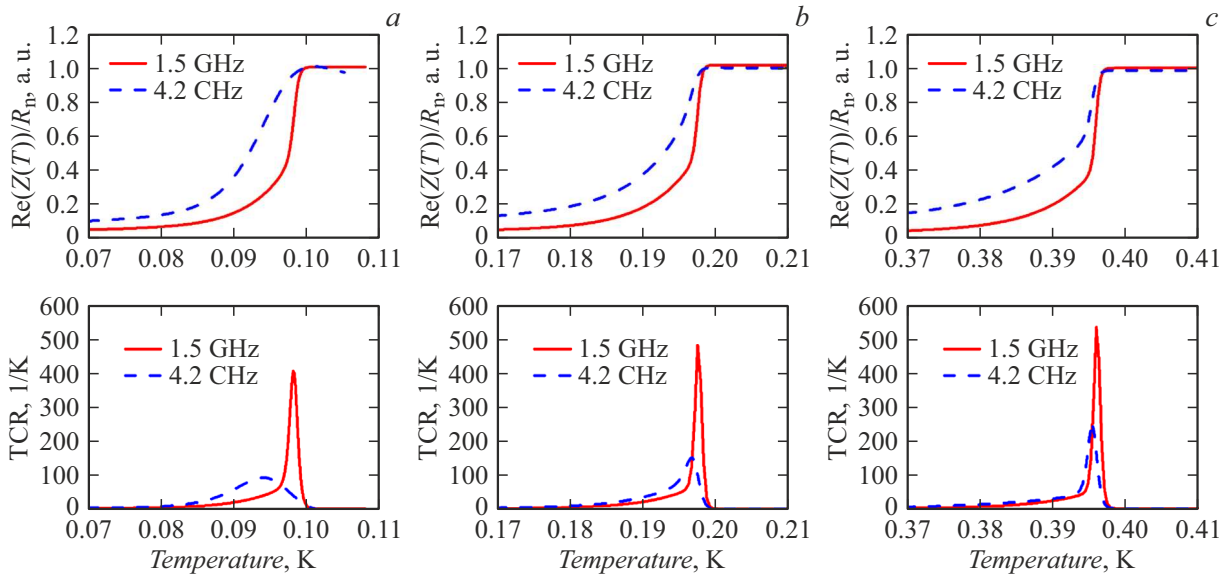

Figure 3. Normalized dependences of the resistive component of nonlinear impedance Re(Z(*T*)) calculated using the Mattis- Bardeen theory [20] for hypothetical equivalent of the superconducting hafnium film having different critical temperatures for two different frequencies: 1.5 and 4.2 GHz (upper row). Temperature coefficient of resistance TCR = $d\mathrm{Re}(Z(T))/dT$ (lower row) was calculated for the same critical temperatures: 100 (*a*), 200 (*b*), and 400 mK (*c*). For comparison, all dependences are given within the temperature range of 40 mK. It is shown that the TCR degradation on Tc at 1.5 GHz may be neglected.

the film does not demonstrate the superconducting state; 2) resistive (non-superconducting) contact of the bridge in the electrode overlapping area; 3) full absence of the conducting contact between the bridge and one or both niobium electrodes due to the interface contamination. The first and second consequences result in weak and indistinguishable resonance because the resonator is damped so much that its amplitude is very small and the band is incomparably wider that the expected one. The third case should result in the resonance shift to higher frequencies that are beyond the operating range of the 1.35–1.6 GHz buffer amplifier used in the system. It was decided to modify the absorber, in particular, to replace a small microbridge contact area by a wide hafnium underlayer as shown in Figure 4 in order to avoid the effect of contacts or at least to make the induced impedance low due high capacity of such overlap. The same approach was used in the niobium prototype at the early research stage [14,16,17].

The measurements gave a somewhat unexpected and interesting result. Critical temperature of the hafnium film was about 210 mK and an effect occurred that can be explained by high kinetic inductance that was not observed before. As the carrier level increases, the resonance curve becomes asymmetric already at low powers and is characterized by soft nonlinear resonance that is quite sensitive to the black-body radiation and, similar to MKID, reacts to the physical heating and irradiation with the shift to the low frequency only (Figure 5).

Figure 5 shows that the left slope of the resonance curve is extremely steep dS_{21}/df and, therefore, the detector demonstrates the power gain (input power to the carrier

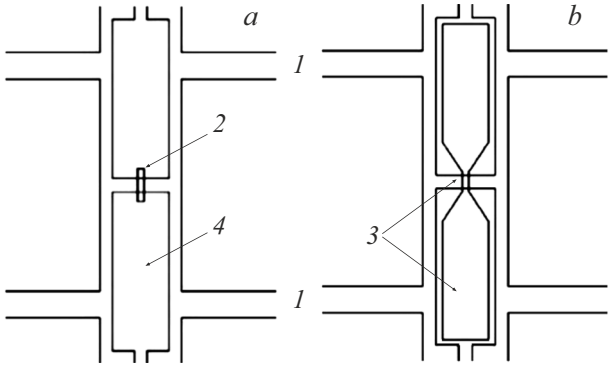

Figure 4. Topology of two options of the contact between the hafnium film and niobium electrodes as part of the same terahertz double-slot antenna (top view, solid lines show the film boundaries); only part of antenna (*1*) is shown (see Figure 2): *a* — 50 nm hafnium film (*2*) as a short 2 × 2 μm bridge connecting the niobium electrodes with 2 × 2 μm overlap; *b* — hafnium film (*3*) that forms the same bridge, but broadening under the niobium electrodes (*4*).

power increment) more than 10 dB (Figure 6). Such RFTES behavior may be explained qualitatively by the reduction (disappearance) of the Andreev mirror effect [22].

It was expected that due to the proximity effect between the hafnium sublayer and the covering niobium film, superconductivity enhancement in hafnium will take place, and the Andreev mirrors at the input electrode boundary will be kept at least at the bias frequency of about 1.5 GHz. If there are no mirrors on such boundary, then the quick

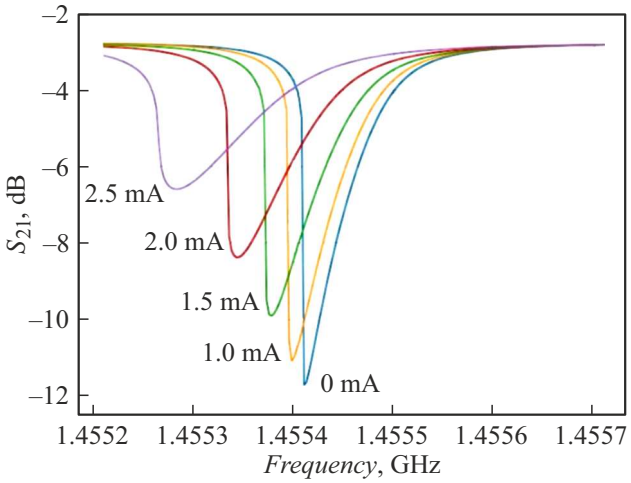

Figure 5. RFTES detector response with high kinetic inductance effect to the optical signal from the black-body radiation source in the black body heating current range 0–2.5 mA (optical signal power $P_s = 0 - 1$ pW) [19]. The swept carrier power at the chip input is constant, −80 dBm (10 pW), chip temperature is 70 mK.

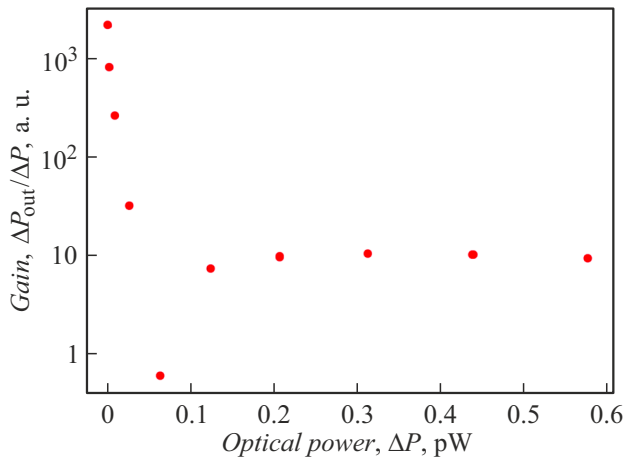

Figure 6. Conversion gain ratio of the black-body (BB) radiation (Optical Power) measured for the black body temperature range 1–10 K. The output power is the carrier power variation at a fixed frequency 1.4554 GHz. The optical power calibration was performed as described in [19] considering the Planck formula. The resonance dip shifts as shown in Figure 5, and for the BB radiation lower than 0.1 pW, at frequency 1.4554 GHz falls on the steep left slope of the resonance curve (Gain is higher), and for high powers — to the right more gardual slope (Gain is lower). The detector output power increment has opposite signs depending on the minimum position $S_{21}(f)$ relative to the carrier frequency; the absolute value of such increment, ΔP_{out}, was used to draw the data.

removal of hot electrons from the small bridge volume to the larger hafnium volume under the electrodes takes place and heating of the electronic subsystem in the bridge area becomes impossible (inefficient). It is logical to assume that the increase in the current density in the shrink (bridge) area results in the kinetic effect. It is known that the MKID concept is built on unpairing without heating, i.e. with small number of non-equilibrium (hot) electrons, meaning that $2\Delta/h \leq f_s$ (f_s — is the signal frequency). In other words, almost all photon energy is spent to break a pair and negligibly small part of energy is left for thermal interaction with quasiparticles. In our case, due to low hafnium gap energy, this condition is not satisfied, and $2\Delta/h \approx 20\,\text{GHz} \leq f_s \approx 650\,\text{GHz}$ is the actual case. Large hafnium film volumes under the niobium electrodes are presumably absorbers of the energetic quasiparticles that are generated in the bridge because the difference between the signal photon and gap energies is high. If such interpretation is valid, then the wide sublayer helps avoid increasing in the density of non-equilibrium quasiparticles in the bridge that is favorable in terms of the MKID concept. Note that in our case such outflow of hot (non-equilibrium) quasiparticles appears not only at the terahertz signal frequency f_s, but also at the low carrier frequency f_c.

Thus, the absorber reconfiguration detected a strong kinetic effect that achieves its maximum nonlinear shape — soft resonance with hysteresis and slope $dS_{21}/df \to \infty$ at the incident frequency of about 1.5 GHz, demonstrating quite moderate heating of the electronic subsystem in the hafnium-based film microbridge. Summing up, the new experimental data support the existence of the Andreev mirrors in case of short bridges, which was discussed previously [15,18], and the unusual kinetic mode of RFTES with new absorber configuration deserves more detailed study.

The experiment data enable some theoretical estimates for which equivalent RFTES circuit diagrams as shown in Figure 7 may be used. The kinetic inductance increment L_k at $T = 70$ mK may be estimated by the shift of the resonator frequency with respect to its low-power position using the data from Figure 5 and electromagnetic RFTES model shown in Figure 7, b in low loss approximation ($Y_b \to 0$).

The experiment has shown that at low carrier power $P_c \approx -105$ dBm (on chip), nonlinear effect is low and the resonance curve S_{21} is symmetric at a frequency near $f_c = 1.45545$ GHz. Calculation using the EM model shown in Figure 7, *b* estimates the bridge current as 0.33 μA. When an increased carrier power $P_c \approx -80$ dBm is applied to the chip, the current through the bridge is about 6 μA, and distortion is observed — shift of the lower resonance point downwards in frequency by about 50 kHz (Figure 5, curve 0 mA), which, according to the calculation, corresponds to the additional bridge inductance $dL_{k1} \approx 0.11$ nH. The same frequency shift is provided by the optical power $P_{s1} \approx 0.15$ pW, when low nondistorting carrier power $P_c \approx -105$ dBm is used. At $P_{s2} \approx 1$ pW (curve 2.5 mA, Figure 5), additional inductance occurs for which the EM model predicts $dL_{k2} \approx 0.33$ nH. Approximately the same frequency shift occurs when the chip temperature increases up to $T \approx 200$ mK, which is close to the critical bridge temperature. Using these data, the superconducting carrier concentration n_s may

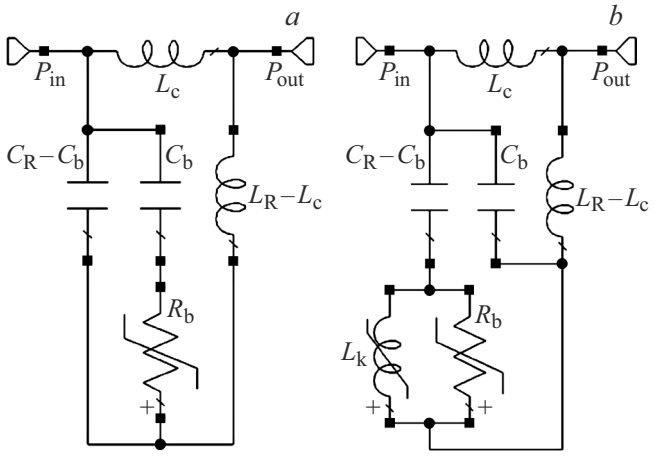

Figure 7. Simplified equivalent circuit diagrams of *C*-type RFTES detector chip: *a* — in resistive approximation; *b* — in terms of kinetic effect described by the nonlinear inductance L_k. The terahertz antennas shown in Figure 1 are not shown herein for clarity. Resonator frequency is defined by L_R and C_R, and the dip in the carrier transmission depends on by the coefficient of coupling with the excitation line, which is defined by inductor L_c. For *C*-type RFTES, the resonator Q factor is set using the current divider $C_b/(C_R - C_b)$. It should be noted that the input/output terminals on the chip are interchangeable.

be solved and the kinetic effect model may be verified. The known relation for the kinetic inductance of a square thin superconducting film for the fixed concentration of superconducting carriers n_s:

$$L_{k\square}(n_s) = \frac{m}{n_s e^2 d}, \tag{1}$$

It is obvious that the inductance increment is caused by concentration variation due to unpairing of the superconducting carriers exposed to terahertz photons. It should be noted that the experimental film has the equal width and length, i.e. 1 square (Figure 4, *b*). Let's estimate the concentration variation dn_s using the experimentally calculated inductance increments $dL_{k\square}$ for the 0.15 pW and 1 pW optical signal as discussed above:

$$\frac{dL_{k\square}}{dn_s} = -\frac{m}{n_s^2 e^2 d}. \tag{2}$$

The optical power can be written as the photon flux N_{ph} with a mean frequency in the antenna range of about 650 GHz: $N_{ph2} \approx 2.3 \cdot 10^9\,s^{-1}$ for $P_{s2} = 1$ pW that, considering the bridge geometry (volume), gives the photon flux density $n_{ph2} \approx 2.58 \cdot 10^{18}\,s^{-1}\cdot cm^{-3}$. For 0.15 pW, the photon flux will be $N_{ph1} \approx 3.5 \cdot 10^8\,s^{-1}$, and the flux density will be $n_{ph2} \approx 1.74 \cdot 10^{18} s^{-1}\cdot cm^{-3}$. We assume that all photons are absorbed by the superconducting carriers which are unpaired and, without the Andreev mirrors, the excess heat is quickly removed by quasiparticles from the bridge volume. The number of simultaneously excited (unpaired) superconducting carriers will depend on the excited state lifetime τ that will be defined by the recombination time. This time is assumed equal to the electron-phonon interaction time and for $T = 200$ mK, $\tau_2 \approx 0.2$ ms, and for $T = 100$ mK, $\tau_1 \approx 1$ ms may be assumed. This means that with shorter recombination time (with shorter lifetime of hot quasiparticles), the transfer process will involve fewer pairs than the number of photons arriving per second, and the concentration variation effect will be lower

$$n_{ph}\tau = dn_s. \tag{3}$$

The system of equations for the two obtained kinetic inductance increments dL_{k1} and dL_{k2} can be written for corresponding photon concentrations, and solved for n_s:

$$L_k(n_s - n_{ph1}\tau_1) - L_k(n_s) = dL_{k1},$$

$$L_k(n_s - n_{ph2}\tau_2) - L_k(n_s) = dL_{k2}. \tag{4}$$

Solution (4) gives quite low concentration of superconducting carriers $n_s \approx 3.4 \cdot 10^{18}\,cm^{-3}$. It is important that solution of system of equations (4) depends on the selected parameters $\tau_1(100\,\text{mK})$ and $\tau_2(200\,\text{mK})$ which do not contradict the known experimental data, for example [23]. It should be also noted that the experimentally obtained inductive response caused by the optical action of the same power does not depend on the carrier power, which proves the independent action on the electronic subsystem of the carrier at approx. 1.5 GHz and of the signal at approx. 650 GHz. As the carrier power increases, only the resonance curve symmetry varies: the lower frequency slope becomes steeper and the upper slope becomes more gentle, which is also inevitably reflected on the conversion gain ratio dS_{21}/dT that may exceed 10 dB. Thus, we have demonstrated the effective nonlinear kinetic inductance mode in the detector built according to other rules than MKID, but having similar and even higher transfer characteristics.

We may compare the MKID and RFTES mode noise of our detector. The nonlinear kinetic inductance is directly associated with the variation of the superconducting carrier concentration, i.e. a stochastic process of Copper pair disintegration and recombination takes place and is accompanied with the electronic noise of non-thermal origin. The MKID concept includes a condition of quite small-size film (the size of about the free electron path) where the gap energy is lower than in the electrodes and where superconducting carriers as well as relaxing quasiparticles are locked within the absorber, that is obviously not satisfied in the case of our „MKID“. In the locked volume with low gap energy, heating of the electronic subsystem is inevitable, which is, on the one hand, favorable for unpairing with participation of the terahertz photons (RFTES concept), but, on the other hand, heating stimulates the accumulation of thermal quasiparticles and „dark“ unpairing due to the carrier power, which contradicts the MKID concept. The same spurious effects limit the carrier level required for resonator excitation and reading the MKID state. Summing up, the RFTES and

MKID modes have contradictory optimization conditions that cannot be implemented for the same material at the same temperature. This complicates direct comparison of the two types of detectors.

Invasive reading is the basis of the RFTES technology, however, in the MKID concept, invasive action to the resonator results in occurrence of excessive recombination noise known as the fundamental restriction on NEP (on threshold sensitivity) MKID [24–26]:

$$NEP_{GR} = 2\Delta\sqrt{\frac{N_{eq}}{\tau_{qp}}},$$

$$N_{eq} = n_0 V. \quad (5)$$

For RFTES with a short bridge, another noise statistics is assumed: near T_c, the Copper pair concentration is low and the gap energy is also low, which allows to neglect the recombination noise compared with the thermal noise of normal electrons in the electron gas mode. For RFTES, the main component will be sufficient - the NEP-term defined as the thermal noise of the electron gas:

$$NEP_{RFTES} = \sqrt{4GT_e^2 k_B},$$

$$G = n\Sigma N_{eq} T_e^n \quad (6)$$

and then estimate the MKID and RFTES sensitivity ratio as

$$\alpha = \frac{NEP_{GR}}{NEP_{RFTES}} = \frac{2\Delta}{\sqrt{4n\Sigma T_e^n T_e^2 k_B \tau_{qp}}}, \quad (7)$$

n_0 is the concentration (density) of equilibrium quasiparticles within the bridge V; Σ is the material parameter $(12.5 \pm 2) \cdot 10^8$ W/(m^3·K^6); exponent n in our experiments was $n = 5$ [18]. It should be noted that the thermal noise is also present in MKID, but is not included in (7). The estimates show that $\alpha \approx \Delta_{MKID}/\Delta_{RFTES}$, i.e. RFTES noise is lower in the case of operating temperature of the absorber is the same.

In addition it should be noted that the invasive reading signal for both detectors results in generation of quasiparticles by the reading photons. This causes the increase in N_{eq}, but also in noise induced by the carrier photons (photon NEP of the carrier). Since the recombination noise is essential for MKID, as low as possible powers are used for reading (non-invasive or minimally invasive reading), which imposes high requirements for the noise temperature of the used semiconductor amplifier T_{LNA}. Remember that both types of detectors are the carrier modulators, i.e. the linear power transducers [W/W]. The higher the carrier power and the higher the intrinsic noise of the amplifier $\propto \sqrt{P_c \cdot T_{LNA}}$ are, the worse the amplifier-induced NEP is. However, the noise value (NEP) reduced to the detector input is inversely proportional to the detector conversion gain ratio that grows linearly as the carrier power increases, that is obvious at the specified modulation depth and specified signal power. Thus, invasive reading may be favorable for suppression of the NEP amplifier $\propto \sqrt{T_{LNA} \cdot P_c}$, if the growth of the conversion gain ratio of the detector itself is considered. This fits to the idea of the thermal action of the carrier used to shift the effective temperature of the RFTES electronic subsystem, i.e. to set the temperature higher than the substrate temperature towards the optimum temperature near T_c.

4. Stability and thermal oscillations

Instability of thermal and current mode in superconducting films is usually manifested in abrupt switching from the superconducting state to the resistive state or back, often accompanying with thermal hysteresis. Study of stability of the superconducting thermometer film read with direct current in middle of the superconducting phase transition $0 < R(T) < R_n$ was an important stage in the development of the classical TES detector [18]. It is known that for stabilization in this area, negative electrothermal feedback is required, which is equivalent to the voltage mode that can be implemented with a low-resistance shunt [3]. For the classical TES, such shunt is usually implemented in hybrid way, i.e. at some distance from the thermometer or even outside the chip, to avoid spurious heating of the absorber. This condition hampers (limits) the use high reading frequencies because the hybrid (wire) connection circuit may become distributed and the impedance may become frequency-dependent, which results in the loss of the voltage mode. In this context, integral connection with the resonator is a benefit of RFTES because it is used to obtain a pre-calculated bridge insertion impedance with high accuracy and provides an opportunity to define a stable operation mode even with positive electrothermal feedback, i.e. to achieve considerable amplification [15,16].

An interesting feature of RFTES is the self-oscillations in the form of the carrier power modulation, which was found even in the all-niobium electromagnetic demonstrator and first described in [18]. Such phenomenon was also reported in hafnium samples due to their ageing, i.e. it may be qualitatively explained by the critical current at the boundary of the bridge and niobium electrodes. We managed to build a mathematical model where the carrier current may achieve the critical current of the superconducting interface in the point of bridge connection to the electrodes, and series resistance ΔR_n appears in the circuit in a stepwise manner. This results in transition of a high-Q resonator to a new state with lower Q factor and lower bridge heating, but is accompanied by a heat pulse. When absorber cools down, the new steady-state condition and the current become lower than the critical current, then superconductivity is restored and the system comes to the start of the cycle at a rate defined by the new resonator Q factor. Thus, we most probably deal with new type of relaxation oscillation.

It is interesting that the frequency of such oscillations are of order of 10 kHz in the experiment being dependent on the thermal power applied to the absorber, and their

power is averaged at the detector output and no NEP degradation is observed. Assuming that the spectral line width of an oscillator is defined by the noise power, the observed spectrum width of such oscillations is defined by the noise whose level agrees with NEP measured by a traditional method as the power dispersion. Mathematical model of such oscillations is discussed in [27] and supports the experimental data with reasonable accuracy.

5. Potential applications

A matrix imaging sensor is the most demanded applied RFTES option [28]. Traditional design with individual lens antennas, for example [29,30], implies the filling coefficient of the field of view of about 0.25, i.e. 4 exposures are required to get the full picture. This is attributed to the optical system geometry when the effective lens aperture diameter is equal to only half-distance between the optical axes of the adjacent pixels. Solution for a more dense pixel packing may be found by creating a multiple-beam antenna when several antennas made on a single chip are installed in the focal plane of the immersion lens [18,31,32]. However, it is difficult to arrange antennas from figure 2 as a closely packed group due to the extended structural part near the open end of the resonator where the antenna is placed. To implement the denser packing, an alternative approach may be used with inductive connection of the bridge to the resonator (L-type detector), that is illustrated in Figure 8. L-type detectors have no extended structure near the antenna, and a compact group of seven pixels may be configured as shown in Figure 9.

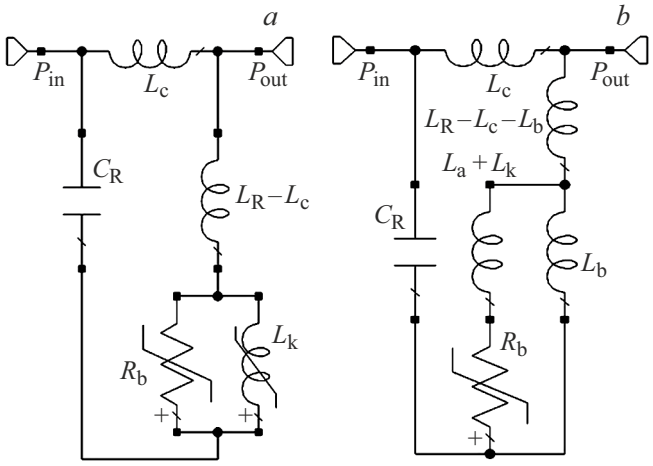

Figure 8. Simplified equivalent circuit diagrams of the detectors with absorber R_b in the inductive circuit of the resonator: a — MKID sensor, b — L-type RFTES detector considering the antenna inductance effect, L_a, and kinetic effect, L_k. The terahertz antennas connected to the absorber are not shown to clarify the idea. Resonator frequency is defined by L_R and C_R, coefficient of coupling with the excitation line is defined by the inductor L_c. For the L-type RFTES detector (b), the resonator Q factor is set using the voltage divider, $L_b/(L_R - L_c - L_b)$.

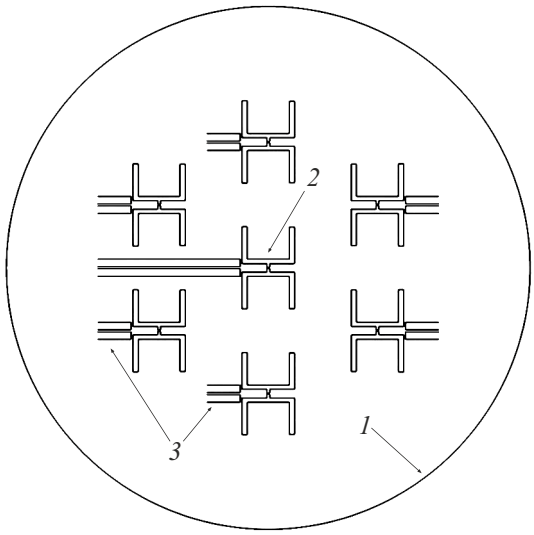

Figure 9. Simplified chip layout of the matrix consisting of seven closely packed RFTES detector antennas on the common immersion lens using the L-type coupling element between the resonator and absorber (L-detectors). Antennas are located within the circle (*1*) approx. 1 mm in diameter and can be easily placed near the optical center (*2*) of the immersion lens 10 mm in diameter, which does not introduces significant distortions into the symmetry of their beam patterns [31]. For clarity, only connection lines between the antennas and resonators (*3*) are shown, that is similar Figure 2.

Another interesting application of the L- and C-detector concept is integration of two detectors into a differential configuration [33] (Figure 10). Absorption balance of two microbridges in a single resonator makes it possible to record only the difference in power of signals arriving at their antennas. This concept is based on the effect of the same loss applied by the L- and C-absorbers into the common resonator, but different signs of dS_{21}/dT, which leaves the resonator Q factor unchanged, if the same signals apply to both detectors. When such method is used for two adjacent pixels with minimum possible spacing on chip, then detection of the radiation gradients (boundaries) may become much more efficient.

Further development area of the RFTES technology is in modification of the concept of two resonator loads to create an active detector described conceptually in [34,35], where the dc SQUID similar to [36] is integrated into the resonator as L-absorber of the differential detector. This provides the match between the SQUID amplifier and resonator which current amplitude is controlled by the C-type RFTES detector. Thus, noise-immune parametrical signal amplification can be implemented to achieve quantum sensitivity of the whole device.

The THz-frequency black-body radiation source method, in terms of the signal circuit theory, may be implemented similarly to the popular matched load method, which uses a coaxial cable in the GHz range [37]. This follows from the fact that the role of the cable is limited to channeling

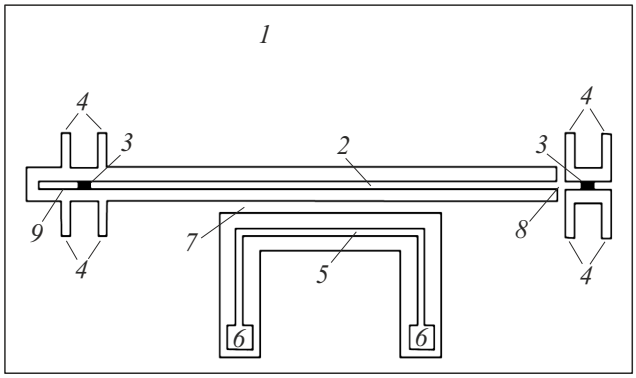

Figure 10. Simplified layout of the differential detector chip containing two RFTES structures: *C*-type (left-hand) and *L*-type (right-hand). On substrate (*1*), there is resonator (*2*) loaded with two bridges-absorbers (*3*) using end coupling capacitor (*9*) and coupling inductor (*8*). terahertz antennas (*4*), excitation line (*5*) with contacts (*6*) and magnetic coupling (*7*), which provide heating of both bridges to the optimum temperature near T_c.

the microwave noise currents of the matched load towards the sensor in a similar way as a rectangular waveguide used for the same purpose. A quasi-optical beam formed by the lens antenna is one of the radiation channeling method, but without using waveguiding surfaces. Since the size of the matched load inserted in the waveguiding circuit of the planar antenna (Figure 2) does not play any significant role, its size may be considered as lumped, and the heated bridge in the resonator can also serve as a source of thermodynamic power emitted by the lens antenna into free space. This concept allowing heat production to be reduced dramatically and modulation rate of the black-body terahertz calibrator to be increased is developed in the experimental study [38].

Conclusion

The RFTES detector concept has undergone several verification stages, including the response and sensitivity measurement using classical procedures, including optical measurements with terahertz thermodynamic sources, and demonstrated good agreement with the initial theoretical predictions. The detected high-performance kinetic response mode shall be additionally investigated. Promising RFTES-based devices are imaging matrices that may be operated using the existing MKID sensor matrix operation procedures. The RFTES technology may be used to create thermodynamic radiation sources and a set of new integral devices such as a differential detector and active detector with built-in parametric amplifier. Therefore, the development of the RFTES technology is a very promising applied research area.

Acknowledgments

The study was supported by „Quantum Internet“ project No. K2-2022-029 within the Startegic Academic Leadership Program „Priority-2030“, and by grant No. 24-29-20298 of the Russian Science Foundation.

Conflict of interest

The authors declare that they have no conflict of interest.

References

[1] J. Clarke, P.L. Richards, N.H. Yeh. Appl. Phys. Lett., **30**, 664 (1977). https://doi.org/10.1063/1.89278
[2] D.E. Prober. Appl. Phys. Lett., **62**, 2119 (1993). https://doi.org/10.1063/1.109445
[3] J.S. Lee, J. Gildemeister, W. Holmes, A. Lee, P. Richards. Appl. Opt., **37** (16), 3391 (1998). https://doi.org/10.1364/AO.37.003391
[4] K.D. Irwin, G.C. Hilton. Topics Appl. Phys., **99**, 63 (2005). https://doi.org/10.1007/10933596_3
[5] N. Bluzer. J. Appl. Phys., **78**, 7340 (1995). https://doi.org/10.1063/1.360383
[6] P.K. Day, H.G. LeDuc, B.A. Mazin, A. Vayonakis, J. Zmuidzinas. Nature, **425**, 817 (2003). https://doi.org/10.1038/nature02037
[7] B.S. Karasik, W.R. McGrath, H.G. LeDuc, M.E. Gershenson. Supercond. Sci. Tecnol., **12**, 745 (1999). https://doi.org/10.1088/0953-2048/12/11/316
[8] A. Shurakov, Y. Lobanov, G. Goltsman. Supercond. Sci. Technol., **29** (2), 023001 (2016). https://doi.org/10.1088/0953-2048/29/2/023001
[9] S.V. Shitov. Tech. Phys. Lett., **37** (10), 932 (2011). https://doi.org/10.1134/S1063785011100117
[10] T.M. Lanting, H.M. Cho, J. Clarke, W.L. Holzapfel, A.T. Lee, M. Lueker, P.L. Richards, M.A. Dobbs, H. Spieler, A. Smith. Appl. Phys. Lett., **86**, 112511 (2005). https://doi.org/10.1016/j.phpro.2012.02.476
[11] K.D. Irwin, K.W. Lehnert. Appl. Phys. Lett., **85**, 2107 (2004). https://doi.org/10.1063/1.1791733
[12] Electronic media. Available at: https://www.premwave.com/microwave-components/frequency-meters.php
[13] B.S. Karasik. *Private Communications* (2011)
[14] A. Kuzmin, S.V. Shitov, A. Scheuring, J.M. Meckbach, K.S. Il'in, S. Wuensch, A.V. Ustinov, M. Siegel. IEEE Trans. Terahertz Sci. Techn., **3** (1), 25 (2013). https://doi.org/10.1109/TTHZ.2012.2236148
[15] A.V. Merenkov, T.M. Kim, V.I. Chichkov, S.V. Kalinkin, S.V. Shitov. FTT, **64** (10), 1404 (2022). (in Russian) https://doi.org/10.21883/FTT.2022.10.53081.50HH
[16] S.V. Shitov, N.N. Abramov, A.A. Kuzmin, M. Merker, M. Arndt, S. Wuensch, K.S. Ilin, E.V. Erhan, A.V. Ustinov, M. Siegel. IEEE Trans. Appl. Supercond, **25** (3), (2014). https://doi.org/10.1109/TASC.2014.2385090
[17] A.V. Merenkov, V.I. Chichkov, A.B. Ermakov, A.V. Ustinov, S.V. Shitov. IEEE Trans. Appl. Supercond., **27** (4), 1 (2017). https://doi.org/10.1109/TASC.2017.2655507

[18] A.V. Merenkov, V.I. Chichkov, A.B. Ermakov., A.V. Ustinov, S.V. Shitov. IEEE Trans. Appl. Supercond., **28** (7), 282798110 (2018). https://doi.org/10.1109/TASC.2018.2827981
[19] T.M. Kim, A.V. Merenkov, An.B. Ermakov, L.S. Solomatov, V.I. Chichkov, S.V. Shitov. ZhTF, **93** (7), 995 (2023). (in Russian). https://doi.org/10.21883/JTF.2023.07.55759.117-23
[20] D.C. Mattis, J. Bardeen. Phys. Rev., **111**, 412 (1958). https://doi.org/10.1103/PhysRev.111.412
[21] N.N. Abarmov. Tech. Phys., **61** (2), 2, 202 (2016). https://doi.org/10.1134/S106378421602002X
[22] A.F. Andreev. ZhETF, **46** (5), 1823 (1964). (in Russian).
[23] E.M. Gershenzon, M.E. Gershenzon, G.N. Gol'tsman, A.M. Lyul'kin, A.D. Semenov, A.V. Sergeev. Sov. Phys., **97** (3), 901 (1990).
[24] A. Sergeev, M. Reizer. Int. J. Mod. Phys. B, **10**, 635 (1996). https://doi.org/10.1142/S021797929600026X
[25] M.E. Gershenson, D. Gong, T. Sato, B.S. Karasik, A.V. Sergeev. Appl. Phys. Lett., **79**, 2049 (2001). https://doi.org/10.1063/1.1407302
[26] A.V. Sergeev, V.V. Mitin, B.S. Karasik, Appl. Phys. Lett., **80**, 817 (2002). https://doi.org/10.1063/1.1445462
[27] L.S. Solomatov, A.V. Merenkov, S.V. Shitov. *Teoreticheskoe issledovanie avtokolebaniy v RFTES-detektore. Nanofizika i nanoelektronika.* Tr. XXVIIII Mezhdunar. simp. (IFP RAN, Nizhny Novgorod, 11–15 marta 2024 g.), t. 1, 560 s. ISBN 978-5-8048-0123-7
[28] M.D. Audley, W.S. Holland, W.D. Duncan, D. Atkinson, M. Cliffe, M. Ellis, X. Gao, D.C. Gostick, T. Hodson, D. Kelly, M.J. MacIntosh, H. McGregor., T. Peacocke, I. Robson, I. Smith, K.D. Irwin, G.C. Hilton, J.N. Ullom, A. Walton, C. Dunare, W. Parkes, P.A.R. Ade, D. Bintley, F. Gannaway, M. Griffin, G. Pisano, R.V. Sudiwala, I. Walker, A. Woodcraft, M. Fich, M. Halpern, G. Mitchell, D. Naylor, P. Bastien. Nucl. Instrum. Methods Phys. Res. A, **520**, 479 (2004). https://doi.org/10.1016/j.nima.2003.11.378
[29] G.B. Rebeiz. Proceed. IEEE, **80**, 11 (1992). https://doi.org/10.1109/5.175253
[30] Electronic source. Available at: https://www.tydexoptics.com/
[31] M. Kominami, D.M. Pozar, D.H. Schaubert. IEEE Trans. Ant. Propag., AP-33, 600 (1985). https://doi.org/10.1109/TAP.1985.1143638
[32] A.V. Uvarov, S.V. Shitov, A.N. Vystavkin. Uspekhi sovremennoy radioelectroniki, **8**, 43 (2010).
[33] S.V. Shitov (Patent RF na izobretenie №2801920 ot 28 dekabria 2022)
[34] S.V. Shitov. ZhTF, **93** (7), 988 (2023). (in Russian). https://doi.org/10.21883/JTF.2023.07.55758.116-23
[35] N.Yu. Rudenko, S.V. Shitov. *Razrabotka aktivnogo teragertsovogo RFTES-detektora. Nanofizika i nanoelektronika.* Tr. XXVIIII Mezhdunar. simp. (IFP RAN, Nizhny Novgorod, 11
[35] –15 marta 2024 g.), t. 1, 560 s. ISBN 978-5-8048-0123-7
[36] G.V. Prokopenko, S.V. Shitov, D.V. Balashov, P.N. Dmitriev, V.P. Koshelets, J. Mygind. IEEE Trans. Appl. Supercond., **11** (1), 1239 (2001). https://doi.org/10.1109/TASC.2003.814146
[37] T.M. Kim, S.V. Shitov. Pis'ma v ZhTF, **47** (24), 13 (2021). (in Russian) https://doi.org/10.21883/PJTF.2021.24.51791.18897
[38] T.M. Kim, V.I. Chichkov, S.V. Shitov. *Issledovanie termodinamicheskogo izluchatelya s SVCh razogrevom dlya kalibrovki RFTES-detektora. Nanofizika i nanoelektronika.* Tr. XXVIIII Mezhdunar. simp. (IFP RAN, Nizhny Novgorod, 11–15 marta 2024 g.), t. 1, 560 s. ISBN 978-5-8048-0123-7

Translated by E.Ilinskaya